

## The neuroprotective role of melatonin against amyloid $\beta$ peptide injected mice

J. GUNASINGH MASILAMONI<sup>1,2</sup>, E. PHILIP JESUDASON<sup>1,3</sup>, S. DHANDAYUTHAPANI<sup>1</sup>, BEN S. ASHOK<sup>4</sup>, S. VIGNESH<sup>1</sup>, W. CHARLES. E. JEBARAJ<sup>5</sup>, SOLOMON F. D. PAUL<sup>6</sup>, & RAJADAS JAYAKUMAR<sup>1</sup>

<sup>1</sup>Bio-Organic and Neurochemistry Laboratory, Central Leather Research Institute, Adyar, Chennai, India, <sup>2</sup>Department of Neurology, Yerkes National Primate Research Center, Emory University, Atlanta, GA, USA, <sup>3</sup>Department of Comparative and Biomedical Sciences, School of Veterinary Medicine, Louisiana State University, Baton Rouge, USA, <sup>4</sup>Department of Biochemistry, <sup>5</sup>Department of Biotechnology, and <sup>6</sup>Genetics Research Cell, Sri Ramachandra University, Porur, Tamil Nadu, Chennai, India

Accepted by Dr J. Keller

(Received 7 February 2008; revised 14 June 2008)

### Abstract

Widespread cerebral deposition of a 40–42 amino acid peptide called amyloid  $\beta$  peptide ( $A\beta$ ) in the form of amyloid fibrils is one of the most prominent neuropathologic features of Alzheimer's disease (AD). The clinical study provides evidence that accumulation of protofibrils due to the Arctic mutation (E22G) causes early AD onset. Melatonin showed beneficial effects in an AD mouse model. Mice were divided into four different groups ( $n = 8$  per group): (i) control group, (ii) scrambled  $A\beta$ -injected group, (iii)  $A\beta$  protofibril-injected group and (iv) melatonin-treated group. A single dose of (5  $\mu$ g)  $A\beta$  protofibril was administered to the  $A\beta$  protofibril-injected and melatonin-treated groups via intracerebroventricular injections. The results demonstrate that melatonin treatment significantly reduces  $A\beta$  protofibril-induced reactive oxygen species (ROS) production, intracellular calcium levels and acetylcholinesterase activity in the neocortex and hippocampus regions. Based on these findings it is suggested that melatonin therapy might be a useful treatment for AD patients.

**Keywords:** *Alzheimer's disease, amyloid  $\beta$  peptide, protofibril, astrocytes, reactive oxygen species, antioxidant, calcium, acetylcholine*

### Introduction

Alzheimer's disease (AD), a neurodegenerative disorder among the elderly population, is characterized clinically by progressive loss of memory and cognition. The pathological hallmarks of AD are senile plaques and neurofibrillary tangles in the neocortex and hippocampus. One of the main constituents of senile plaques is insoluble amyloid  $\beta$  peptide ( $A\beta$ ), which is an important factor in the neuropathology observed in AD [1]. However, AD propagation is better correlated

with the presence of soluble oligomer not amyloid plaques [2,3]. Recently, Lesne et al. [4] reported accumulation of soluble dodecamer amyloid aggregate in Tg2576 mice and administration of these isolated amyloid aggregates to rats lead to memory deficits. *In-vitro* studies demonstrate that neuronal cells are more vulnerable to soluble oligomers; amyloid derived diffusible ligands (ADDLs) and protofibrils than to fibrils [5–7]. In addition, several groups have clearly demonstrated that  $A\beta$  protofibrils have electrophysiological effects on neurons [7]. Strong clinical evidence

Correspondence: Dr R. Jayakumar, Head & Sr. Asst. Director, Bio-Organic and Neurochemistry Laboratory, Central Leather Research Institute, Adyar, Chennai 600 020, India. Tel: 9144-24911386, ext 324. Fax: 9144-24911589. Email: karkuvi77@yahoo.co.uk

indicates that  $A\beta$  protofibril generation induced by the Arctic mutation (E22G) causes early AD onset found in a Swedish family with hereditary AD [8]. However, the biochemical mechanism involved in the protofibril-induced toxicity is not very well addressed.  $A\beta$  protofibrils are described as >100 kDa curved linear structures with a diameter of  $\sim 5$  nm and a length of up to 200 nm, which remain soluble upon centrifugation at 16 000–18 000 g [9–12].

Besides  $A\beta$  deposition, selective neuronal loss is another hallmark of AD brains. For example, AD is associated with dysfunction and degeneration of basal forebrain cholinergic neurons [13]. One of the characteristic changes that occurs in AD is an increase in the activity of acetylcholinesterase (AChE), within and around amyloid plaques [14]. This increase promotes the assembly of amyloid beta-peptides into toxic protofibrils and causes enhanced cytotoxicity of these peptides [15]. However, the cause for the dysfunction of basal forebrain cholinergic neurons and its relationship to  $A\beta$ -peptides has yet to be determined. These reports suggest that AChE could play a pathogenic role in AD by influencing the process leading to amyloid toxicity.

Numerous studies have shown that levels of the pineal hormone melatonin decrease during the ageing process [16,17] and those patients with AD have more profound reductions of melatonin [18]. In addition, melatonin reduces the secretion of soluble amyloid  $\beta$  [19] and may prophylactically reduce the amyloid  $\beta$  protein aggregation and oxidative stress in the AD mouse model [20–22]. In the present study, we chose to investigate the mechanistic aspects of melatonin's protective function on  $A\beta$  protofibril-triggered neurotoxicity. Interestingly, we found that melatonin prevents the toxic insults produced by amyloid protofibrils. Our data suggest that melatonin

therapy might be an ideal drug of choice for AD patients.

## Materials and methods

Male Swiss albino mice weighing 30–35 g were obtained from Tamil Nadu Veterinary and Animal Sciences University (Madhavaram, Chennai, Tamil Nadu, India). The animals were maintained in Poly-acrylic cages under hygienic conditions at normal room temperature (28–30°C) on a 12 h light/dark cycle. Mice were fed a commercial pellet diet (Hindustan lever Ltd, Bangalore, India). The animals had free access to water. The whole surgical procedure was performed in a laminar flow hood under aseptic conditions following NIH animal ethical guidelines and following approval by the animal care committee of Central Leather Research Institute, Chennai, Tamilnadu.

### Synthesis and purification of $A\beta_{1-42}$

The peptide  $A\beta_{1-42}$  and scramble  $A\beta_{42-1}$  were synthesized by manual solid phase chemistry, using Fmoc as the protective group for N-terminal ends and 1-Hydroxy benzotriazole (HOBt) and N, N-dicyclohexyl-carbodiimide as coupling agents and Penta fluoro phenol as activators of carboxylic ends. The peptides were cleaved from (4-Hydroxymethylphenoxy acetyl) Wang resin with trifluoromethane sulphonic acid/thioanisole/ethanedithiol/trifluoroacetic acid (1:1:1:7) and precipitated with cold ether. The composition of peptides was determined by amino acid analysis using the Phenyl isothiocyanate (PITC) method. The purified peptides were characterized by MALDI-TOF MS analysis (Figure 1A). The peaks corresponding to the  $(M+2H)^+$  ion of

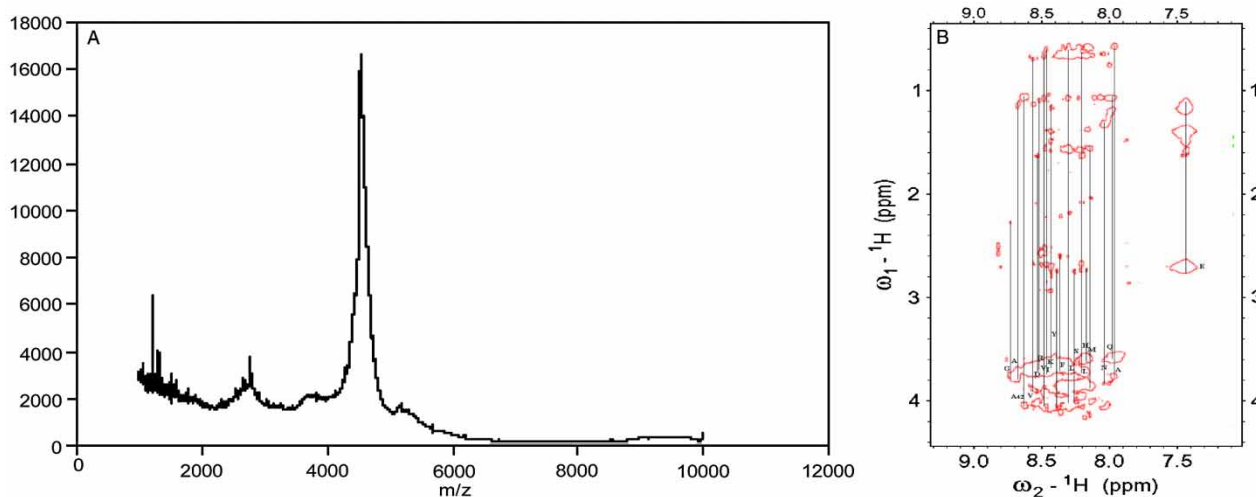


Figure 1. (A) Matrix-assisted laser desorption/ionization (MALDI) spectra of  $A\beta_{1-42}$ . Aliquots of 0.5  $\mu$ l were applied on to the MALDI target and allowed to air dry as described under esis and Purification of  $A\beta_{1-42}$ . (B) The TOCSY for  $A\beta_{1-42}$ . The sample concentration was 1 mM of the peptide, in phosphate buffer (pH 7.4). The experiments were performed with samples in 90%  $H_2O$  and 10%  $D_2O$  (v/v).

the  $A\beta_{1-42}$  and  $A\beta_{42-1}$  were observed. The derived mass of the peptides was calculated from the MALDI spectrum to be 4515.4 Daltons. The peptides were then characterized by TOCSY. It was performed on the 800 MHz Varian Unity Plus spectrometer housed in the Stanford NMR Facility (Stanford University, CA). The sample concentration was 1 mM of the  $A\beta_{1-42}$  peptide, in phosphate buffer (pH 7.4). The experiments were performed with samples in 90%  $H_2O$  and 10%  $D_2O$  (v/v) (Figure 1B).

All reagents used in peptide synthesis: Pentafluorophenol (purchased from Spectrochem Pvt. Ltd, Mumbai), N,N-dicyclohexyl carbodiimide (Sigma-Aldrich), Fmoc-AA (Novabiochem), HoBt (Sigma-Aldrich), TFA (Sigma-Aldrich) were of the purest analytical grade. The  $A\beta_{1-42}$  fibrils were formed by solubilizing the peptide in sterile double distilled (DD) water (1 mg/ml) and then incubated 24 h at 37°C [23]. The protofibrillar form thus obtained was used fresh for the present study.

#### *Intracerebroventricular injection of $A\beta_{1-42}$*

$A\beta_{1-42}$  administration was performed according to the procedure established by Laursen and Belknap [24]. Briefly, each mouse was injected with 5  $\mu$ l of  $A\beta_{1-42}$  (concentration of 5  $\mu$ g) at a depth of 2.4 mm bregma using a 50  $\mu$ l Hamilton microsyringe fitted with a 26-gauge needle.

#### *Experimental design*

The animals were divided in to three groups, each group consisting of eight animals, as follows:

- Group I: (control) 5  $\mu$ l of physiological saline was given intracerebroventricularly to mice.
- Group II: (scrambled) 5  $\mu$ g  $A\beta_{42-1}$  was given intracerebroventricularly to mice.
- Group III: ( $A\beta$  protofibril injected) 5  $\mu$ g  $A\beta_{1-42}$  protofibril was given intracerebroventricularly to mice.
- Group IV: (melatonin treated) Melatonin (50 mg/kg body weight) was administered intraperitoneally for 5 days, immediately after the injection of  $A\beta_{1-42}$  protofibrils to the mice.

Animals were decapitated after 5 days. The neocortex and hippocampus were carefully excised and the tissues were stored at  $-70^\circ\text{C}$ . Tissue was weighed and homogenized in 0.1 M Tris buffer pH 7.4. The homogenate was then centrifuged at 5000 g for 10 min ( $4^\circ\text{C}$ ) and the supernatant was used for all the estimations.

#### *Isolation of astrocytes*

Astrocytes were isolated from the forebrains of the control and experimental mice as described by Abe

and Saito [25], which includes 20% of glial and neuronal cells. In brief, 100 mg of forebrain tissue was removed from experimental animals and minced with a scalpel in a solution containing 20  $\mu$ g/ml DNase and 0.3% BSA in Hank's buffered salt solution (HBSS). This was centrifuged and incubated in a solution containing 0.025% trypsin, 0.1% collagenase and 0.3% BSA in HBSS in a water bath at 37°C. After 15 min the resulting mixture was centrifuged and the pellet was agitated five times with a Pasteur pipette. Supernatant was collected after 4 min. The initial viability of astrocytes was greater than 90% as assessed by trypan blue exclusion. Approximately  $8.5 \times 10^6$  cells/ml were used immediately for ROS quantification.

#### *Measurement of intracellular ROS formation*

Formation of intracellular peroxides was detected by fluorescence spectroscopy using a non-fluorescent compound DCFH<sub>2</sub>-DA, which is de-esterified within cells by endogenous esterase to the acid 2',7'-dichlorofluorescein (DCFH<sub>2</sub>), as previously described. The ionized free acids are trapped within the cells and are capable of being oxidized to fluorescent 2',7'-dichlorofluorescein (DCF) by hydroperoxides, although other mechanisms of oxidation cannot be ruled out [26]. An aliquot of 200  $\mu$ l of isolated cells ( $\sim 8.5 \times 10^6$  cells/ml) were made up to a final volume of 2 ml in normal phosphate buffered saline (pH 7.4), to which 100  $\mu$ l of DCFHDA (200  $\mu$ M) was added, and incubated at 37°C for 30 min. Fluorescent measurements were done with excitation and emission filters set at  $485 \pm 10$  nm and  $530 \pm 12.5$  nm, respectively. Results were expressed as percentages; increase in fluorescence was calculated using the following formula  $[(F_{t_{30}} - F_{t_0})/F_{t_0} \times 100]$ , where  $F_{t_0}$  and  $F_{t_{30}}$  are the fluorescence intensities at 0 and 30 min.

ROS production was also observed using a fluorescence microscope. The cells were viewed under a FITC filter with an image analysis system. The images were captured at 40 $\times$  magnification.

#### *Intracellular $Ca^{2+}$ determination*

The isolated astrocytes were immediately loaded with FURA-2AM (1  $\mu$ M) for 45 min, rinsed three times in a HEPES buffer (25 mM HEPES; 125 mM NaCl; 5.9 mM KCl; 1.28 mM  $CaCl_2$ ; 1.1 mM  $MgCl_2$ ) and allowed to equilibrate for 20 min in HEPES medium at room temperature. The cells were rinsed again, resuspended in HEPES medium at the concentration of  $0.5 \times 10^6$  cells/ml and transferred to a cuvette for the measurement of calcium. The cytoplasmic  $Ca^{2+}$  concentration ( $[Ca^{2+}]_i$ ) was measured by dual wavelength spectrophotometry using FURA-2AM as an indicator and a Perkin-Elmer LS-45 luminescence spectrophotometer, as previously described by Ahren [27], the excitation wavelength was continuously

altered between 340–380 nm and the emission wavelength was 490. The  $[Ca^{2+}]_i$  was calculated from the recorded fluorescence ratios of 350/380 nm using the formula described previously by Grynkiewicz et al. [28].

#### Antioxidant enzyme assays

**Superoxide dismutase (SOD) activity.** SOD activity was assayed according to the method of Misra and Fridovich [29]. The assay is based on the inhibition of the epinephrine- adrenochrome transition by the enzyme.

**Catalase activity.** The activity of catalase was determined by the method of Beers and Sizer [30]. The breakdown of hydrogen peroxide on addition of enzyme is followed by observing the decrease in light absorption of peroxide solution in the ultraviolet (UV) region.

**Glutathione peroxidase (GPx).** GPx activity was determined by the method of Rotruck et al. [31] with slight modifications. This method is based on the reaction between glutathione remaining in the following reaction with Dithio-bis-nitrobenzoic acid (DTNB) to form an intermediate, which has absorption maxima at 412 nm.

**Total reduced glutathione (GSH).** The method of Moron et al. [32] was followed to determine total reduced glutathione. The method is based on the reaction of glutathione with DTNB to give absorption at 412 nm.

#### Protein content

Protein content of the homogenates was determined by the method of Lowry et al. [33] using bovine serum albumin as standard.

**In vitro  $H_2O_2$  scavenging assay.** To study the  $H_2O_2$  scavenging ability of melatonin in the *in vitro* condition, we carried out the following assay: astrocytes were isolated from the A $\beta$  protofibril injected mice after 5 days. Approximately  $8.5 \times 10^6$  cells/ml (13 mg cell protein/ml) were incubated at 37°C in an oxygen saturated Tris-buffer (25 mM, pH 7.4) supplemented with 114 mM NaCl, 4.5 mM KCl, 0.7 mM  $MgSO_4$ , 0.3 mM  $CaCl_2$ , 27.8 mM glucose and 12.2 mM  $NaHCO_3$ . The initial viability of astrocytes was greater than 90% as assessed by Trypan Blue exclusion. The isolated astrocytes were divided into two groups; (a) untreated and (b) 10  $\mu$ g melatonin treated groups (the concentration (10  $\mu$ g) was obtained by serial dilution). After 24 h of incubation, ROS, catalase, GPx and GSH were analysed in the untreated and melatonin-treated astrocytes.

**Glucose.** Brain glucose level was estimated by the o-toluidine colour reaction of Dubowski modified by Matsui and Sasaki [34]. The glucose reacts readily with o-toluidine reagent in the presence of acid to form a coloured complex, which has absorption maxima at 640 nm.

**Acetylcholinesterase (AChE) activity.** The activity of AChE was measured based on the method developed by Ellman et al. [35]. This method employs acetylthiocholine iodide (ATChI) as a synthetic substrate for AChE. ATChI is broken down to thiocholine and acetate by AChE and thiocholine, which is reacted with dithiobisnitrobenzoate (DTNB) to produce a yellow colour. The quantity of yellow colour, which develops over time, is a measure of the activity of AChE and was measured at 412 nm.

**Acetylcholine (ACh).** Acetylcholine was estimated by the following procedure of Hestrin [36]. Hydroxylamine at alkaline pH rapidly converts acetylcholine into hydramic acid, which is a direct indicator of acetylcholine content; this was measured at 540 nm.

**Histology.** Tissues used for histological analysis were fixed in 10% neutral buffered formalin. The specimens were processed for routine histopathology. Samples were dehydrated through a graded series of alcohol and xylene. Serial sections were stained with hematoxylin and eosin for histological analysis.

#### Immunohistochemical analysis of GFAP and NF $\kappa$ B.

Under deep anaesthesia, the experimental animals were perfused transcardially with ice-cold paraformaldehyde solution (4% in phosphate buffer, pH 7.4). The neocortex was post-fixed for 4 h and cryoprotected with 18% sucrose solution for 48 h. Neocortices were cut in 10  $\mu$ m-thick sections and placed in phosphate buffered saline (PBS) containing 0.1% sodium azide and stored at 4°C until used for immunohistochemical evaluation for the reactive astrocyte markers glial fibrillary acidic protein (GFAP) and nuclear factor kappa B (NF $\kappa$ B).

GFAP was detected by means of a mouse monoclonal mouse antibody (1:1000 dilution; Oncogene Research Products). NF $\kappa$ B (p65, Rel A) (Ab-1) was detected by means of a rabbit polyclonal antibody (1:500, Oncogene Research Products).

**Interaction between A $\beta$  and melatonin.** Synthetic A $\beta$  peptides were solubilized in DD water at the concentration of 4 mg/ml and the pH adjusted to 7.4. Melatonin was dissolved in buffer A, i.e. 25 mM Tris-HCl and 1 mM EGTA, pH 7.4. 50  $\mu$ M of A $\beta$ , 50  $\mu$ M melatonin and their combination of 1:1 were allowed to incubate at 37°C for 5 days. After 5 days, A $\beta$  fibril formation was assessed by Th-T fluorescence [37]. Stock A $\beta$  peptide solutions



(4 mg/ml) which had been prepared in DD water and stored at  $-85^{\circ}\text{C}$  were diluted (1 mg/ml, final concentration) with phosphate buffered saline (PBS; 20 mM sodium phosphate, 0.9% w/v NaCl, pH 7.4) on the day of experimentation. 50  $\mu\text{M}$  of  $\text{A}\beta$ , 50  $\mu\text{M}$  melatonin and their combination of 1:1 were allowed to incubate at  $37^{\circ}\text{C}$  for 5 days. At specific intervals, aliquots (20  $\mu\text{l}$ ) were removed and combined with 5 mM glycine, pH 8.75, containing 2  $\mu\text{M}$  Th-T in a final volume of 2 ml. Fibril formation was then assessed by measuring the sample fluorescence (excitation and emission wavelengths 425 nm and 480 nm, respectively, and excitation and emission band-pass slits 5 and 10 nm) in a Perkin-Elmer LS-45 luminescence spectrophotometer.

### Statistical analysis

Results were statistically evaluated using one-way analysis of variance (ANOVA) with a post-hoc Tukey's test to determine the significant differences among group means. *P*-values less than 0.05 were considered significant. Different superscripts within a row show significant variation between groups; \**p* < 0.05, \$*p* < 0.01, #*p* < 0.001.

## Results

### ROS

Reactive astrocytes participate in the inflammatory response in AD by producing proinflammatory cytokines and free radicals [38]. Therefore, a possible pathology of AD can be viewed by the accumulation of such free radicals during inflammation [39]. In the present study we observed that the intracellular ROS concentration is significantly higher (*p* < 0.05) in the astrocytes of  $\text{A}\beta$  protofibril-injected mice than in control and scrambled-injected mice (Figure 2). Melatonin therapy reduced  $\text{A}\beta$  protofibril-induced ROS production in the mice (Figure 2). Figure 3 gives the comparison between astrocytes with, without and with partial ROS production. Green cells show a positive signal for ROS, which is an index for free radical levels in the cell. The number of cells with green signals and their concomitant intensities were increased in the  $\text{A}\beta$  protofibril-injected mice when compared to control and melatonin-treated groups (Figure 3). This shows that  $\text{A}\beta$  protofibril-induced ROS was attenuated by melatonin therapy.

### Calcium

Several groups have shown that  $\text{A}\beta$  can induce elevations of intracellular free calcium concentrations  $[\text{Ca}^{2+}]_i$  [40] in neurons. Free intracellular calcium is one of the most important messengers for many of the signal transduction pathways of neurons. Alterations in intracellular calcium homeostasis are critically involved in cell death. The present results show

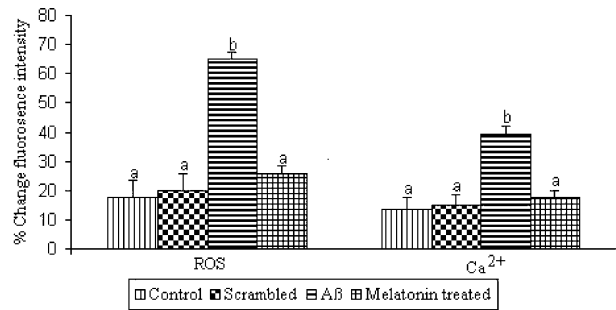


Figure 2. Quantification of ROS generation and intracellular calcium levels in the astrocytes of control, scrambled  $\text{A}\beta_{42-1}$ ,  $\text{A}\beta_{1-42}$  injected and melatonin-treated groups were measured by incubation with DCFH-DA and FURA-2AM for 30 min, at 485 nm and 530 nm, 340–490 using an excitation and emission filter, respectively. Each data point represents the mean of six animals. Bar diagram represents the group mean  $\pm$  SD. Different superscripts indicate significant differences between groups (*p* < 0.05).

that the amyloid protofibril significantly increased the basal intracellular  $\text{Ca}^{2+}$  concentration ( $[\text{Ca}^{2+}]_i$ ) in  $\text{A}\beta$  protofibril-injected mice compared to control mice (*p* < 0.05). Melatonin treatment significantly reduces  $\text{A}\beta$ -induced intracellular  $\text{Ca}^{2+}$  concentration (Figure 2).

### Antioxidant status

There is increasing experimental evidence attributing AD to the impairment in cellular total antioxidant capacity. The activities of the antioxidant enzymes SOD, catalase and Gpx are significantly reduced in the frontal and temporal cortex of AD patients [41]. Our results show that within 5 days amyloid protofibrils impair the antioxidant system in the mice, thereby significantly reducing the activity of these enzymes in the neocortex and hippocampus of  $\text{A}\beta$  protofibril-injected mice (Table I). On the other hand, melatonin treatment protects the antioxidant system from the toxic protofibril insult.

GSH is an important intracellular antioxidant that protects cells against a variety of oxidant species and radicals. The disturbance of GSH homeostasis has been implicated in the pathogenesis of several neurodegenerative diseases, including AD [42]. The present result shows that amyloid protofibril significantly depletes GSH levels in the neocortex and hippocampus of the  $\text{A}\beta$ -induced group when compared with control and melatonin-treated groups (Table I).

### In vitro $\text{H}_2\text{O}_2$ scavenging assay

Astrocytes, together with microglia, are the main effector cells of the innate immune response in the central nervous system (CNS) and can be activated in neurodegenerative diseases to produce an array of inflammatory mediators [4,5]. Excessive production of these inflammatory mediators, which include

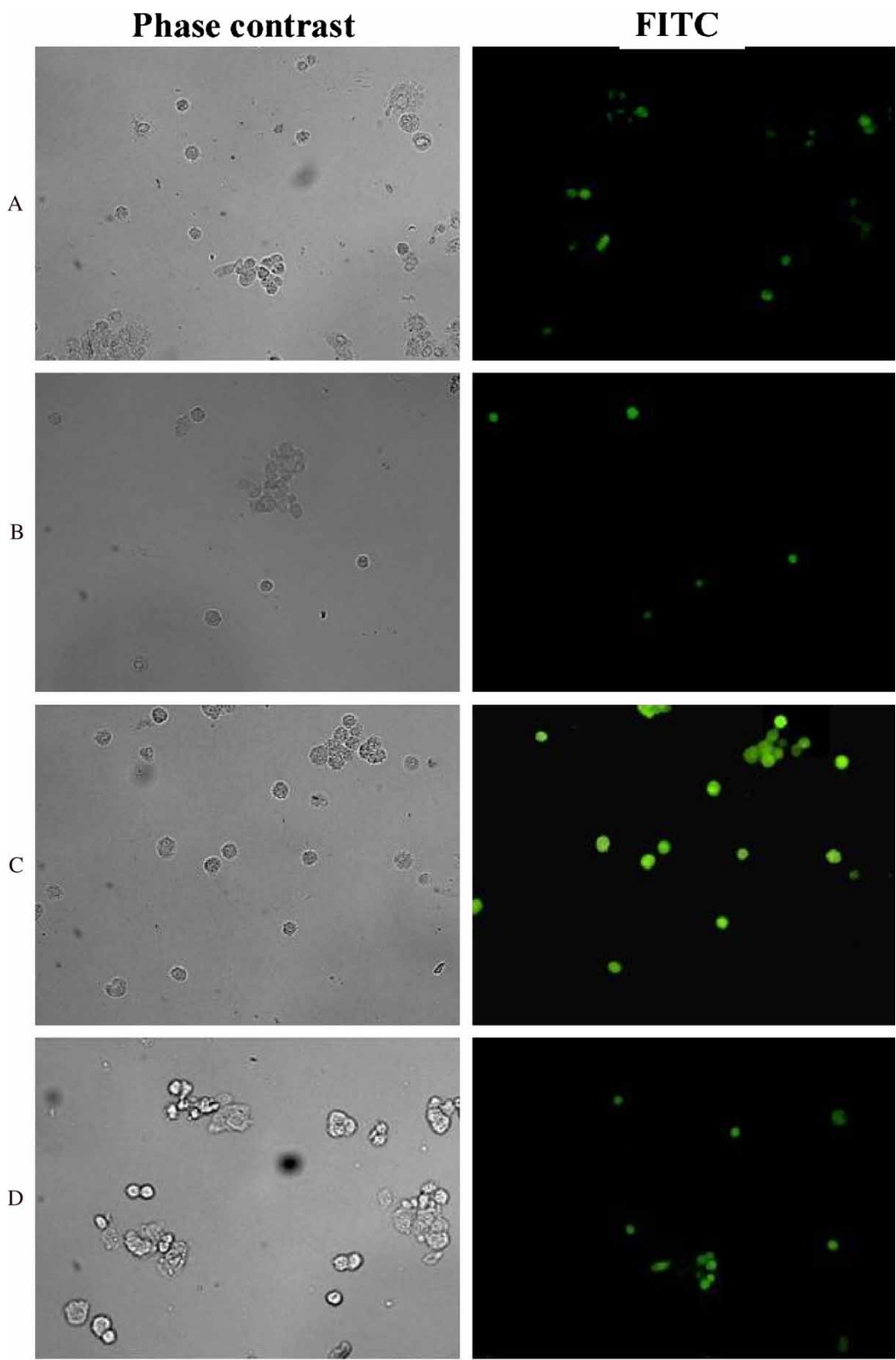


Figure 3. Observation of ROS in the astrocytes, isolated immediately from (A) control, (B) scrambled  $A\beta_{42-1}$ , (C)  $A\beta_{1-42}$  injected and (D) melatonin-treated mice using DCFH-DA as a fluorogenic probe. Cells glowing green is a positive signal for ROS production in FITC filter.

ROS, can contribute to neuroinflammation, which may be responsible for the degeneration of basal forebrain cholinergic cells. A consequence of the

neuroinflammation hypothesis is that selective suppression of neurotoxic products produced by excessive glial activation will result in neuroprotection. To

Table I. Effect of scrambled  $A\beta_{42-1}$ ,  $A\beta_{1-42}$  and melatonin treatment on the levels of antioxidants in the neocortex and hippocampus of mice after 5 days. Values represent the group mean  $\pm$ SD for six animals. Different superscripts within a row show significant variation between groups.

Regions	Parameter	Control	Scrambled	$A\beta$ treated	Melatonin
Neocortex	SOD	0.97 $\pm$ 0.10	0.94 $\pm$ 0.11	0.35 $\pm$ 0.04*	0.81 $\pm$ 0.07
Hippocampus		0.83 $\pm$ 0.07	0.78 $\pm$ 0.08	0.31 $\pm$ 0.04 <sup>s</sup>	0.74 $\pm$ 0.07
Neocortex	Catalase	2.73 $\pm$ 0.26	2.51 $\pm$ 0.23	1.42 $\pm$ 0.13*	2.39 $\pm$ 0.22
Hippocampus		3.54 $\pm$ 0.22	3.51 $\pm$ 0.21	3.26 $\pm$ 0.18 <sup>#</sup>	3.37 $\pm$ 0.18
Neocortex	GPx	43.65 $\pm$ 4.53	41.54 $\pm$ 4.23	32.55 $\pm$ 3.43 <sup>s</sup>	40.24 $\pm$ 3.92
Hippocampus		48.55 $\pm$ 4.18	46.44 $\pm$ 4.22	43.24 $\pm$ 2.79*	47.57 $\pm$ 3.97
Neocortex	GSH	9.52 $\pm$ 0.86	9.21 $\pm$ 0.71	4.03 $\pm$ 0.39 <sup>#</sup>	8.76 $\pm$ 0.81
Hippocampus		12.54 $\pm$ 0.82	11.44 $\pm$ 0.74	7.15 $\pm$ 0.65 <sup>s</sup>	11.36 $\pm$ 0.93

SOD units/min/mg protein, Catalase  $\mu$ moles of  $H_2O_2$  cons/min/mg protein, GPx  $\mu$ moles of GSH cons/min/mg protein, GSH  $\mu$ g/mg protein. \* $p < 0.05$ , <sup>s</sup> $p < 0.01$ , <sup>#</sup> $p < 0.001$ . Units were expressed in Protein.

test this hypothesis, we isolated activated astrocytes from the  $A\beta$  protofibril-injected mice and added melatonin directly to the culture. After 24 h we found that melatonin significantly scavenged  $H_2O_2$  production in the activated astrocyte cultures when compared with control (Figure 4A). In addition, melatonin significantly increased antioxidant levels ( $p < 0.05$ ) in the isolated activated astrocytes (Figure 4B–D). It is interesting to note that that melatonin not only prevents  $A\beta$  protofibril-induced inflammation but also prevents activated-astrocyte-induced secondary inflammation.

#### Glucose

To study the impairment of glucose transporters by  $A\beta$ , we quantified glucose levels in the neocortex and hippocampus of  $A\beta$  injected mice. Reduced glucose uptake occurs early in the AD disease process before neuronal degeneration [43]. The present results show that glucose concentration was significantly reduced in the neocortex and hippocampus ( $p < 0.05$ ) of  $A\beta$ -injected mice when compared to control, scrambled and melatonin-treated groups (Table II). This indicates that melatonin therapy up-regulates glucose

uptake by maintaining continuous metabolism of glucose.

#### Acetylcholine (ACh)/acetylcholine esterase (AChE)

At present the most frequently prescribed anti-Alzheimer's drugs are the AChE inhibitors, which promote memory function and delay the cognitive decline. Inhibition of AChE increases the synaptic levels of acetylcholine and thereby promotes cholinergic neurotransmission. The effect of AChE inhibitors is thus to stabilize and prolong the biological half-life of acetylcholine. Our result shows that addition of protofibril trigger AChE activity in the mice cortex and hippocampus. Melatonin treatment significantly reduced the  $A\beta$  protofibril induced AChE activity in the melatonin-treated group (Table II). In contrast, ACh was significantly decreased in the  $A\beta$ -injected mice when compared to control. Our results show that melatonin treatment protects mice from  $A\beta$ -induced acetylcholine degradation.

#### Histology

The control and scrambled  $A\beta$ -injected groups exhibited normal neocortical architecture, whereas the

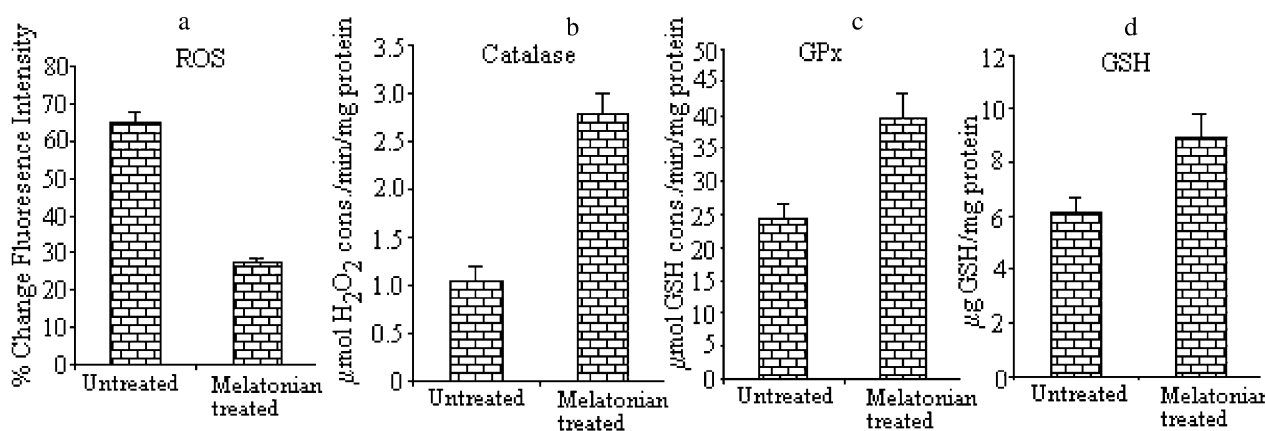


Figure 4. Astrocytes isolated from the  $A\beta$  injected mice were used to study the  $H_2O_2$  scavenging ability of melatonin in the *in vitro* condition. After 24 h of incubation at 37°C (A) ROS level, (B) catalase activity, (C) GPx activity and (D) GSH content were analysed. The data were collected from six independent studies run in duplicate. Bar diagram represents the group mean  $\pm$ SD.

Table II. Effect of scrambled  $A\beta_{42-1}$ ,  $A\beta_{1-42}$  and melatonin treatment on the levels of glucose and acetylcholine and acetylcholine esterase activity in the neocortex and hippocampus of mice after 5 days. Values represent the group mean  $\pm$ SD for six animals. Different superscripts within a row show significant variation between groups.

Regions	Parameter	Control	Scrambled	$A\beta$ treated	Melatonin
Neocortex	Glucose	67.75 $\pm$ 5.19	63.25 $\pm$ 6.21	48.05 $\pm$ 0.11 <sup>*</sup>	65.97 $\pm$ 0.14
Hippocampus		63.83 $\pm$ 6.03	61.75 $\pm$ 6.11	36.52 $\pm$ 3.28 <sup>#</sup>	59.37 $\pm$ 5.18
Neocortex	AChE	65.64 $\pm$ 6.31	60.25 $\pm$ 6.02	97.85 $\pm$ 8.51 <sup>#</sup>	71.84 $\pm$ 6.58
Hippocampus		67.32 $\pm$ 7.08	62.26 $\pm$ 6.09	95.85 $\pm$ 8.74 <sup>§</sup>	64.94 $\pm$ 6.37
Neocortex	ACh	425.86 $\pm$ 31.64	415.77 $\pm$ 37.54	247.03 $\pm$ 20.38 <sup>*</sup>	406.16 $\pm$ 37.88
Hippocampus		432.46 $\pm$ 32.82	422.96 $\pm$ 31.37	251.15 $\pm$ 22.82 <sup>#</sup>	411.36 $\pm$ 33.93

Glucose  $\mu$ g/gm tissue, AChE micromoles acetylthiocholine iodide hydrolysed/min/mg protein, Acetylcholine pmoles/mg protein.

\* $p < 0.05$ , <sup>§</sup> $p < 0.01$ , <sup>#</sup> $p < 0.001$ .

neocortical region of  $A\beta$ -injected brains shows loose oedematous tissue with inflammation and focal rapid astrocytic proliferation (Figure 5C). In contrast, in the melatonin-treated mice; astrocytes appear in a compact neuronal background (Figure 5D).

#### Immunohistochemical analysis of GFAP and NF $\kappa$ B

In the neocortex, immunoreactivity of GFAP, an index of astroglial response to neuronal injury, was increased by inflammation (Figure 6C). Our immunocytochemical analysis of neocortical tissue sections reveals that NF $\kappa$ B, a key factor for the control of cellular pathways involved in inflammation, proliferation and regulation of apoptosis, was increased in cells under oxidative stress (Figure 6G). Melatonin therapy effectively prevented the inflammation-

induced GFAP (Figure 6D) and NF $\kappa$ B immunoreactivities (Figure 6H).

#### Interaction between $A\beta$ and melatonin

To illustrate the direct interaction between melatonin and  $A\beta$  peptide, we have performed the Th-T fluorescence assay. It is well known that Th-T is a dye that specifically binds amyloid-like aggregates and excites at 425 nm and emits fluorescence at 480 nm. Negligible Th-T fluorescence was observed at 480 nm for the  $A\beta$  monomer and  $A\beta$  scrambled peptide. However, 5 days old  $A\beta$  peptide showed the highest Th-T fluorescence, this was prevented by melatonin addition (Figure 7). Here we hypothesized that melatonin directly interacts with  $A\beta$  peptide and thereby prevents its aggregation.

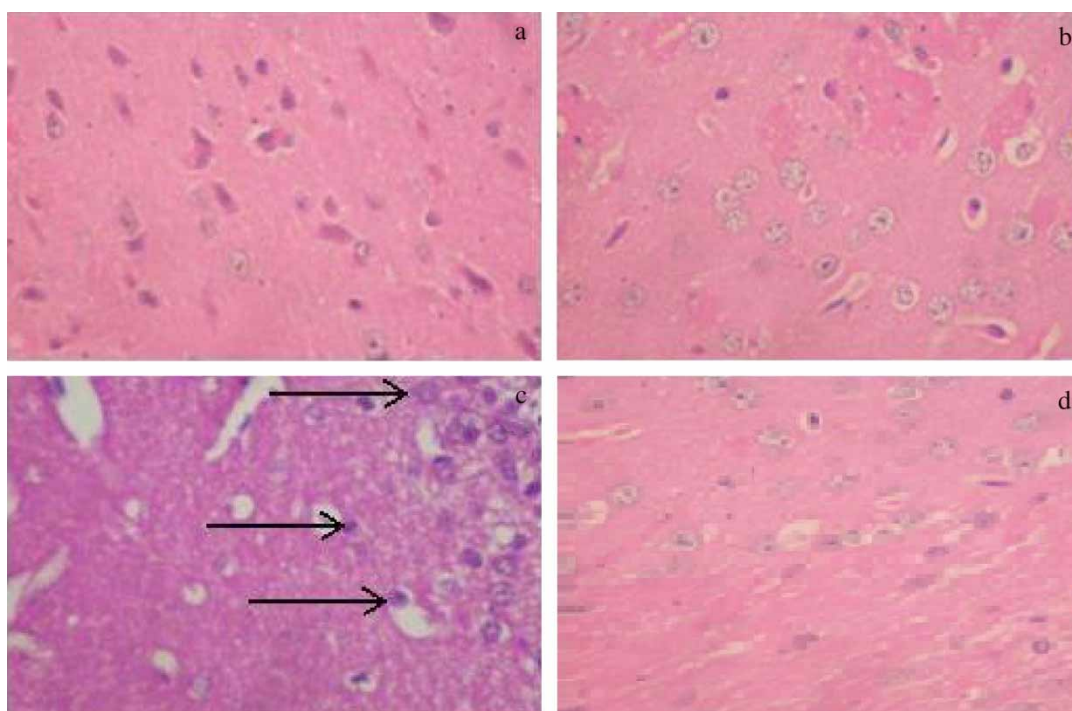


Figure 5. (A) Group I photomicrograph of control neocortex shows astrocytes in a neurofibrillary background. (B) Group II (Scrambled)  $5 \mu$ l  $A\beta_{42-1}$  was given intracerebroventricularly to mice showing normal architecture of control neocortex. (C) ( $A\beta$  injected)  $5 \mu$ l  $A\beta_{1-42}$  was given intracerebroventricularly to mice shows loose oedematous tissue with inflammation and focal rapid astrocytic proliferation. (D) Melatonin-treated neocortex shows astrocytes in compact neuronal background. Scale bar = 100  $\mu$ m.



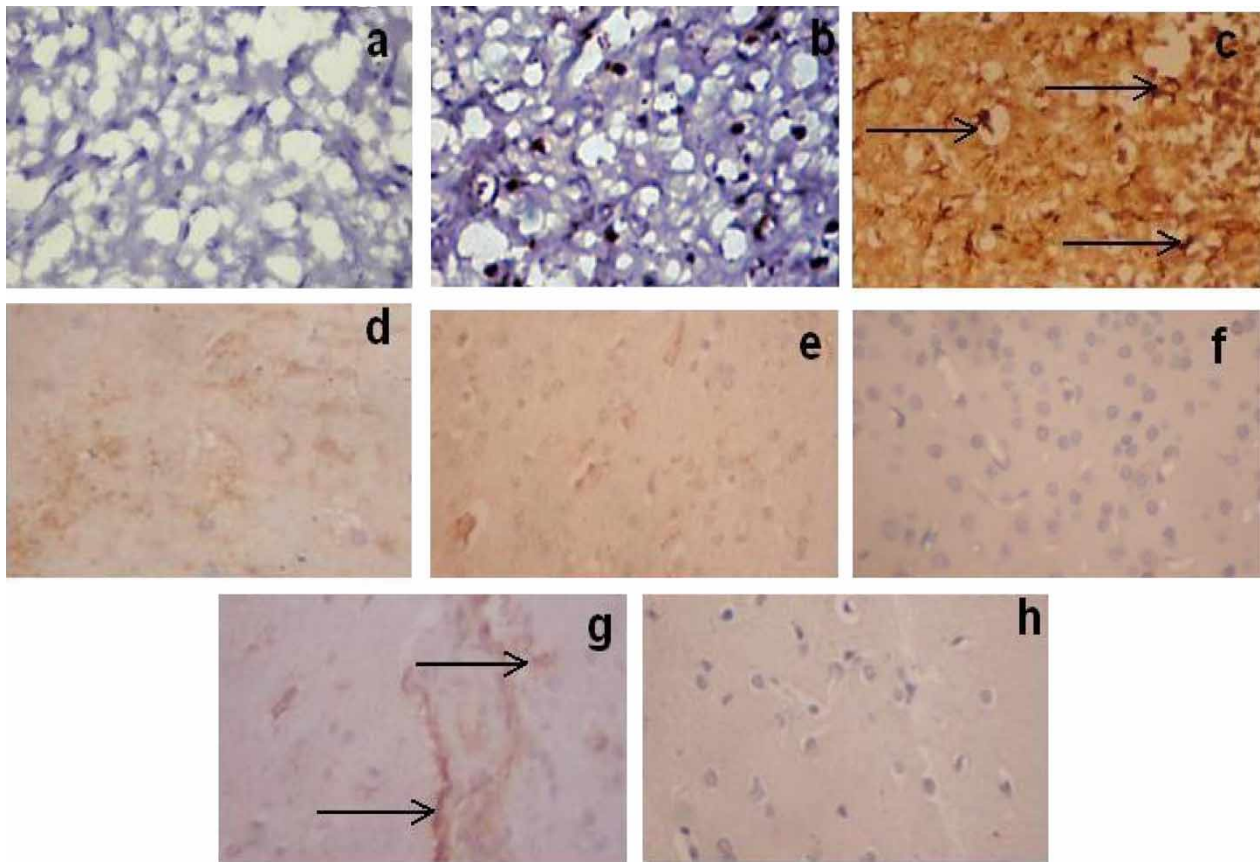


Figure 6. Immunohistochemical staining of GFAP in the neocortex of mice. (A) GFAP expression was absent in the control brain of mice. (B) Group II (Scrambled) 5  $\mu\text{l}$   $A\beta_{42-1}$  was given intracerebroventricularly to mice showing normal architecture. (C) Intense staining with GFAP antibody was observed in the  $A\beta$  treated mice. (D) GFAP expression was prevented by melatonin treatment. (E) Group I  $\text{NF}\kappa\text{B}$  expression was absent in control brain of mice. (F) Group II (Scrambled) 5  $\mu\text{l}$   $A\beta_{42-1}$  was given intracerebroventricularly to mice showing normal architecture. (G) Intense staining with  $\text{NF}\kappa\text{B}$  antibody was observed in the  $A\beta$  treated mice. (H)  $\text{NF}\kappa\text{B}$  expression was prevented by melatonin treatment. Immunohistochemical stain. Scale bar = 100  $\mu\text{m}$ .

## Discussion

Soluble aggregated  $A\beta$  induces oxidative stress in various experimental systems including cultured neurons [44], synaptosomes [45] and endothelial cells [46]. Hartley et al. [7] reported that  $A\beta$  protofibrils significantly alter the electrical activity of neurons as measured by excitatory post-synaptic currents, action potentials and membrane depolarization at low concentrations of protofibrils. Here we have demonstrated that  $A\beta$  protofibrils induce oxidative imbalance in the *in-vivo* mouse model.  $A\beta$  can directly produce  $\text{H}_2\text{O}_2$  by a mechanism that involves the reduction of the metal ions Fe (III) or Cu (II) setting up conditions for Fenton-type chemistry [47]. Melatonin treatment abolished  $A\beta$  protofibril-induced oxidative damage in mice. It is of interest to note that our *in-vitro* fibrillization assay shows that melatonin has great affinity for the  $A\beta$  peptide, which may prevent amyloid fibril formation (Figure 7). Here we hypothesized that melatonin, a free radical scavenger, directly binds with protofibrils, thereby preventing ROS production, and protects neurons from the toxic insults via its antioxidant activities (Figure 3; Table I).

Johnstone et al. [48] reported that soluble  $A\beta$  causes astrocytes to release ROS. This excessive ROS production may contribute to secondary degeneration of basal forebrain neurons. Our *in-vitro* results show that melatonin decreased the protofibril-induced ROS production in astrocytes and reversed the diminished activities of catalase and GPx (Figures 4A–C). Esparza et al. [49] and Kotler et al. [50] observed that melatonin enhances gene expression of anti-oxidative enzymes either under basal conditions or after their inhibition by neurotoxic agents. The stimulation of GSH synthesis by melatonin could be a major antioxidative action of melatonin (Figure 4D). It has been reported that melatonin stimulates the synthesis of the rate-limiting enzyme,  $\gamma$ -glutamylcysteine synthase and thereby increases intracellular GSH concentrations [51].

Our study highlights a significant reduction of glucose levels in the neocortex and hippocampus of  $A\beta$ -injected mice (Table I). Accumulation of free radicals can impair the function of several plasma membrane proteins involved in the maintenance of ion homeostasis, including glucose transporters [52]. Impairment of the glucose transporters leads to ATP

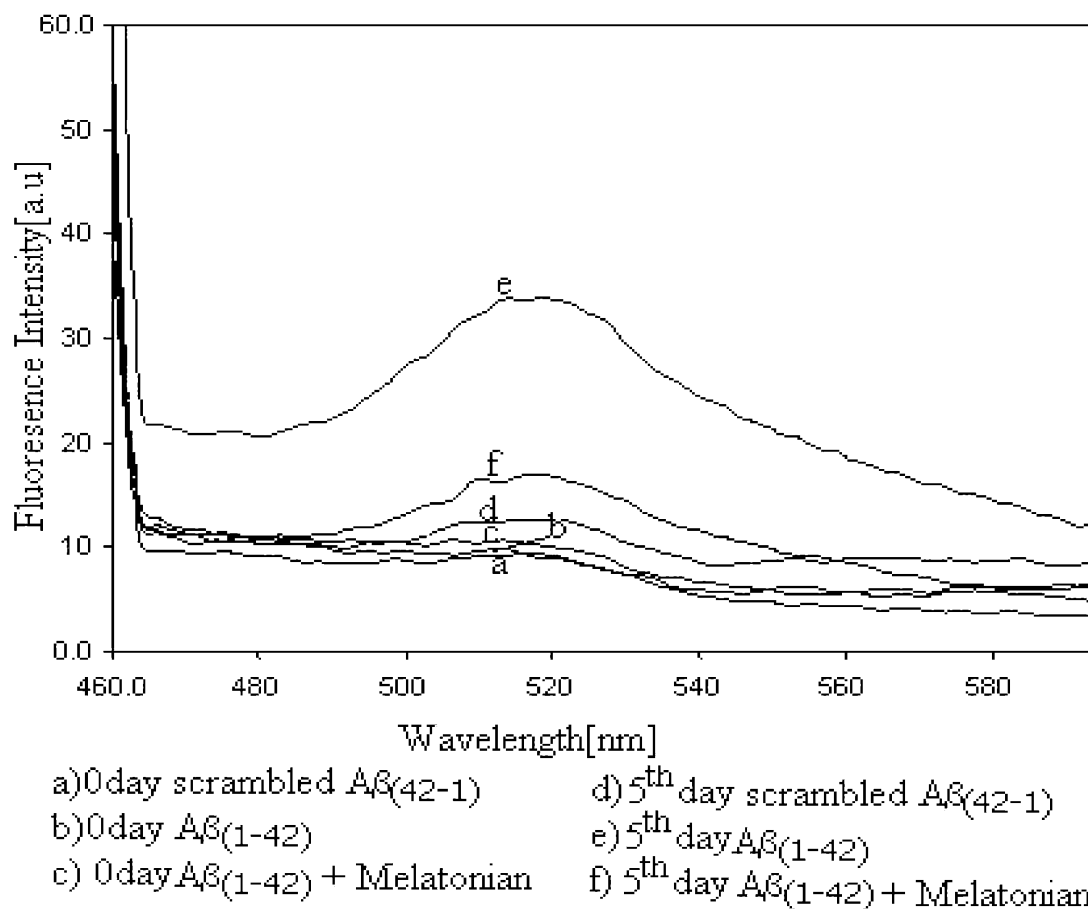


Figure 7. Effects on aggregation of  $A\beta_{1-42}$  by melatonin. The fibril formation of  $A\beta_{1-42}$  was monitored by ThT fluorescence in the absence and presence of melatonin and for scrambled  $A\beta_{42-1}$  alone by incubating at 37°C for 5 days. Fluorescence intensity was measured at excitation wavelength 425 nm and emission wavelength 480 nm.

depletion, which in turn leads to dysfunction of neurons and cell death [53,54]. Treatment with melatonin restored brain glucose levels in the  $A\beta$  protofibril-injected mice, suggesting a possible role for melatonin in scavenging the oxy-radicals and thus maintaining ion homeostasis and preventing the damage of glucose transporters.

There is growing evidence for a possible link between ROS levels and disruption of calcium homeostasis in cell damage and death induced by amyloid peptides [55]. We have also observed an increase in intracellular  $Ca^{2+}$  levels in the  $A\beta$  protofibril-injected mice. Melatonin acts as a protective agent against oxidative damage by scavenging ROS, thereby preventing the  $A\beta$  protofibril-induced  $Ca^{2+}$  homeostasis disruption (Figure 2B).

The degeneration of the forebrain cholinergic pathways is one of the hallmarks of AD and is considered to be the main cause of cognitive impairments [56]. Several studies in AD brains have demonstrated changes in the expression and distribution of AChE [57,58]. We report here that  $A\beta$  protofibrils lead to a significant ( $p < 0.05$ ) increase in AChE activity when compared to control (Table II). Sberna et al. [59]

reported that  $A\beta$  increases AChE activity in P19 cells by increasing calcium entry through L-type voltage-dependent calcium channels, suggesting that the increase in AChE expression around amyloid plaques is a consequence of the disturbance in calcium homeostasis. In our experimental conditions, we have also observed an increase in intracellular  $Ca^{2+}$  levels in the  $A\beta$ -injected mice, which in turn related to the increase in AChE activity. Melo et al. [13] reported that the enhancement of AChE activity induced by  $A\beta$  is mediated by oxidative stress. Our results show that melatonin prevents the enhancement of AChE activity in the  $A\beta$ -injected mice by decreasing ROS production and intracellular calcium levels.

The reduction of ACh in AD brains has been attributed to the neurotoxic effect of  $A\beta$  on cholinergic neurons [60,61]. Our result shows that ACh was significantly reduced in the  $A\beta$  protofibril-injected mice, which might be due to their increased activity of AChE.  $A\beta$  also suppresses ACh synthesis, mainly by increasing ROS production and inhibiting glucose metabolism and thereby reducing the availability of acetyl-CoA for ACh synthesis [62]. Melatonin, a radical scavenger, regulates the glucose level by

enhancing ACh levels in the hippocampus and neocortex of A $\beta$ -injected mice.

Histopathological observations were very well correlated with biochemical changes that occurred in A $\beta$  protofibril-treated mice (Figure 5A–D). The results from the current study show that significantly amplified levels of free radicals were correlated with an obvious decline in the antioxidant defensive enzyme system. The enhanced rate of ROS generation due to the high rate of oxidative metabolism and profusion of polyunsaturated fatty acid (PUFA) in cellular membranes may initiate the reactions that induce oxidative changes [63]. In this regard this study highlights the relationship between antioxidant enzyme dysfunction and A $\beta$ -induced oxidative changes. Epidemiologic studies to confirm the beneficial effects of antioxidants in AD have not yet been conducted.

Astrocytes synthesize and secrete GFAP [64], which is believed to provide structural support to residual tissue in cases of brain injury involving localized cell death and GFAP deposition is often used as a marker of astrocyte immune activation [65]. These glial cells become reactive in response to brain tissue damage caused by ischemia, hypoxia and seizures [66]. Astrocytes and their processes play a role in guiding migration and axonal growth of neurons during embryonic development [67] and in establishing the blood–brain barrier [68]. Furthermore, changes in astrocyte morphology also occur in pathological conditions, a process termed reactive gliosis. Our results show that the GFAP levels were increased in the neocortex of the A $\beta$  group when compared to control (Figure 6C).

NF $\kappa$ B is a ubiquitous transcription factor required for maximal transcription of a wide array of pro-inflammatory molecules, which are thought to be important in the generation of inflammation in A $\beta$  toxicity [69]. Once activated, NF $\kappa$ B dimers are transported to the nucleus, where they stimulate the transcription of genes that carry NF $\kappa$ B DNA binding motifs [70]. Melatonin may protect oxidant-mediated inflammation and tissue damage by virtue of its ability to scavenge free radicals and by inhibiting the activation of NF $\kappa$ B (Figure 6H).

In conclusion, our study reveals that the pineal hormone melatonin directly interacts with A $\beta$  protofibrils and abolishes protofibril-induced ROS production, thereby maintaining intracellular calcium and acetylcholine levels and protecting antioxidant enzymes in neuronal cells. In addition, melatonin rescues antioxidant enzymes and maintains their function. Thus, melatonin therapy may be useful for the amelioration of cholinergic dysfunction in AD.

## Acknowledgements

We are grateful to Jim Bogenpohl, Neuroscience, Emory University, Atlanta, GA, USA for his valuable assistance in scientific corrections. The authors and Dr J. G. M. and Dr E. P. J. thank the Council of Scientific and Industrial Research (CSIR, New Delhi), India for awarding a fellowship. Dr S. D. thanks the Indian Council of Medical Research (ICMR, New Delhi, India) for awarding Senior Research Fellowships. Finally we thank the reviewer's for their imperative comments and valuable suggestions.

**Declaration of interest:** The authors report no conflicts of interest. The authors alone are responsible for the content and writing of the paper.

## References

- [1] Hardy J, Selkoe DJ. The amyloid hypothesis of Alzheimer's disease: progress and problems on the road to therapeutics. *Science* 2002;297:353–356.
- [2] McLean CA, Cherny RA, Fraser FW, Fuller SJ, Smith MJ, Beyreuther K, Bush AI, Masters CL. Soluble pool of Abeta amyloid as a determinant of severity of neurodegeneration in Alzheimer's disease. *Ann Neurol* 1999;46:860–866.
- [3] Lue LF, Kuo YM, Roher AE, Brachova L, Shen Y, Sue L, Beach T, Kurth JH, Rydel RE, Rogers J. Soluble amyloid beta peptide concentration as a predictor of synaptic change in Alzheimer's disease. *Am J Pathol* 1999;155:853–862.
- [4] Lesne S, Koh MT, Kotilinek L, Kaye R, Glabe CG, Yang A, Gallagher M, Ashe KH. A specific amyloid-beta protein assembly in the brain impairs memory. *Nature* 2006;440:352–357.
- [5] Dahlgren KN, Manelli AM, Stine WB Jr, Baker LK, Krafft GA, LaDu MJ. Oligomeric and fibrillar species of amyloid-beta peptides differentially affect neuronal viability. *J Biol Chem* 2002;277:32046–32053.
- [6] Lambert MP, Barlow AK, Chromy BA, Edwards C, Freed R, Liosatos M, Morgan TE, Rozovsky I, Trommer B, Viola KL, Wals P, Zhang C, Finch CE, Krafft GA, Klein WL. Diffusible, nonfibrillar ligands derived from Abeta1–42 are potent central nervous system neurotoxins. *Proc Natl Acad Sci USA* 1998;95:6448–6453.
- [7] Hartley DM, Walsh DM, Ye CP, Diehl T, Vasquez S, Vassilev PM, Teplow DB, Selkoe DJ. Protofibrillar intermediates of amyloid beta-protein induce acute electrophysiological changes and progressive neurotoxicity in cortical neurons. *J Neurosci* 1999;19:8876–8884.
- [8] Nilsberth C, Westlind-Danielsson A, Eckman CB, Condron MM, Axelman K, Forsell C, Stenh C, Luthman J, Teplow DB, Younkin SG, Näslund J, Lannfelt L. The 'Arctic' APP mutation (E693G) causes Alzheimer's disease by enhanced Abeta protofibril formation. *Nat Neurosci* 2001;4:887–893.
- [9] Harper JD, Wong SS, Lieber CM, Lansbury PT. Observation of metastable Abeta amyloid protofibrils by atomic force microscopy. *Chem Biol* 1997;4:119–125.
- [10] Walsh DM, Lomakin A, Benedek GB, Condron MM, Teplow DB. Amyloid beta-protein fibrillogenesis. Detection of a protofibrillar intermediate. *J Biol Chem* 1997;272:22364–22372.
- [11] Paivio A, Jarvet J, Graslund A, Lannfelt L, Westlind-Danielsson A. Unique physicochemical profile of beta-amyloid peptide variant Abeta1–40E22G protofibrils: conceivable



- neuropathogen in arctic mutant carriers. *J Mol Biol* 2004;339:145–159.
- [12] Johansson AS, Berglind-Dehlin F, Karlsson G, Edwards K, Gellerfors P, Lannfelt L. Physicochemical characterization of the Alzheimer's disease-related peptides A beta 1-42Arctic and A beta 1-42wt. *FEBS J* 2006;273:2618–2630.
- [13] Melo JB, Agostinho P, Oliveira CR. Involvement of oxidative stress in the enhancement of acetylcholinesterase activity induced by amyloid beta-peptide. *Neurosci Res* 2003;45:117–127.
- [14] Moran MA, Mufson EJ, Gomez-Ramos P. Colocalization of cholinesterases with beta amyloid protein in aged and Alzheimer's brains. *Acta Neuropathologica* 1993;85:362–369.
- [15] Alvarez A, Alarcon R, Opazo C, Campos EO, Munoz FJ, Calderon FH, Dajas F, Gentry MK, Doctor BP, De Mello FG, Inestrosa NC. Stable complexes involving acetylcholinesterase and amyloid-beta peptide change the biochemical properties of the enzyme and increase the neurotoxicity of Alzheimer's fibrils. *J Neurosci* 1998;18:3213–3223.
- [16] Ferrari E, Arcaini A, Gornati R, Pelanconi L, Cravello L, Fioravanti M, Solerte SB, Magri F. Pineal and pituitary-adrenocortical function in physiological aging and in senile dementia. *Exp Gerontol* 2000;35:1239–1250.
- [17] Reiter RJ. The ageing pineal gland and its physiological consequences. *Bioessays* 1992;14:169–1675.
- [18] Mishima K, Okawa M, Hishikawa Y, Hozumi S, Hori H, Takahashi K. Morning bright light therapy for sleep and behavior disorders in elderly patients with dementia. *Acta Psychiatrica Scand* 1994;89:1–7.
- [19] Lahiri DK. Melatonin affects the metabolism of the beta-amyloid precursor protein in different cell types. *J Pineal Res* 1999;26:137–146.
- [20] Feng Z, Qin C, Chang Y, Zhang JT. Early melatonin supplementation alleviates oxidative stress in a transgenic mouse model of Alzheimer's disease. *Free Radic Biol Med* 2006;40:101–109.
- [21] Matsubara E, Bryant-Thomas T, Pacheco Quinto J, Henry TL, Poeggeler B, Herbert D, Cruz-Sanchez F, Chyan YJ, Smith MA, Perry G, Shoji M, Abe K, Leone A, Grunde-Ikbal I, Wilson GL, Ghiso J, Williams C, Refolo LM, Pappolla MA, Chain DG, Neria E. Melatonin increases survival and inhibits oxidative and amyloid pathology in a transgenic model of Alzheimer's disease. *J Neurochem* 2003;85:1101–1108.
- [22] Jesudason EP, Baben B, Ashok BS, Masilamoni JG, Kirubakaran R, Jebaraj WC, Jabakumar R. Anti-inflammatory effect of melatonin on A beta vaccination in mice. *Mol Cell Biochem* 2007;298:69–81.
- [23] Nielsen EH, Nybo M, Svehag SE. Electron microscopy of prefibrillar structures and amyloid fibrils. *Methods Enzymol* 1999;309:491–496.
- [24] Laursen SE, Belknap JK. Intracerebroventricular injections in mice. Some methodological refinements. *J Pharm Methods* 1986;16:355–357.
- [25] Abe K, Saito H. Menadione toxicity in cultured rat cortical astrocytes. *Jpn J Pharmacol* 1996;72:299–306.
- [26] Cathcart R, Schwiens E, Ames BN. Detection of picomole levels of hydroperoxides using a fluorescent dichlorofluorescein assay. *Anal Biochem* 1983;134:111–116.
- [27] Ahren B. Galanin increases cytoplasmic calcium in insulin-producing RINm5F cells by activating phospholipase C. *Biochim Biophys Res Commun* 1996;221:89–94.
- [28] Grynkiewicz G, Poenie M, Tsien RY. A new generation of Ca<sup>2+</sup> indicators with greatly improved fluorescence properties. *J Biol Chem* 1985;260:3440–3450.
- [29] Misra HP, Fridovich I. The role of superoxide anion in the autoxidation of epinephrine and a simple assay for superoxide dismutase. *J Biol Chem* 1972;247:3170–3175.
- [30] Beers RF Jr, Sizer IW. A spectrophotometric method for measuring the breakdown of hydrogen peroxide by catalase. *J Biol Chem* 1952;195:133–140.
- [31] Rotruck JT, Pope AL, Ganther HE, Swanson AB, Hafeman DG, Hoekstra WG. Selenium: biochemical role as a component of glutathione peroxidase. *Science* 1973;179:588–590.
- [32] Moron MS, Depierre JW, Mannervik B. Levels of glutathione, glutathione reductase and glutathione S-transferase activities in rat lung and liver. *Biochim Biophys Acta* 1979;582:67–78.
- [33] Lowry OH, Rosebrough NJ, Farr AL, Randall RJ. Protein measurement with the Folin phenol reagent. *J Biol Chem* 1951;193:265–275.
- [34] Matsui S, Sasaki T. [Correlation between glacial acetic acid content of O-TB reagents and color reactions]. *Rinsho byori* 1971;19(Suppl):384.
- [35] Ellman GL, Courtney KD, Andres V Jr, Feather-Stone RM. A new and rapid colorimetric determination of acetylcholinesterase activity. *Biochem Pharm* 1961;7:88–95.
- [36] Hestrin S. Acylation reactions mediated by purified acetylcholine esterase. *Biochim Biophys Acta* 1950;4:310–321.
- [37] Walsh DM, Hartley DM, Condron MM, Selkoe DJ, Teplow DB. *In vitro* studies of amyloid beta-protein fibril assembly and toxicity provide clues to the aetiology of Flemish variant (Ala692→Gly) Alzheimer's disease. *Biochem J* 2001;355:869–877.
- [38] Wallace MN, Geddes JG, Farquhar DA, Masson MR. Nitric oxide synthase in reactive astrocytes adjacent to beta-amyloid plaques. *Exp Neurol* 1997;144:266–272.
- [39] Kontogiorgis CA, Xu Y, Hadjipavlou-Litina D, Luo Y. Coumarin derivatives protection against ROS production in cellular models of Abeta toxicities. *Free Radic Res* 2007;41:1168–1180.
- [40] Mattson MP. Metal-catalyzed disruption of membrane protein and lipid signaling in the pathogenesis of neurodegenerative disorders. *Ann N Y Acad Sci* 2004;1012:37–50.
- [41] Aksenov MY, Tucker HM, Nair P, Aksenova MV, Butterfield DA, Estus S. The expression of key oxidative stress-handling genes in different brain regions in Alzheimer's disease. *J Mol Neurosci* 1998;11:151–164.
- [42] Cardoso SM, Oliveira CR. Glutathione cycle impairment mediates A beta-induced cell toxicity. *Free Radic Res* 2003;37:241–250.
- [43] Pettegrew JW, Panchalingam K, Klunk WE, McClure RJ, Muenz LR. Alterations of cerebral metabolism in probable Alzheimer's disease: a preliminary study. *Neurobiol Aging* 1994;15:117–132.
- [44] Sultana R, Newman S, Mohammad-Abdul H, Keller JN, Butterfield DA. Protective effect of the xanthate, D609, on Alzheimer's amyloid beta-peptide (1–42)-induced oxidative stress in primary neuronal cells. *Free Radic Res* 2004;38:449–458.
- [45] Butterfield DA, Hensley K, Harris M, Mattson M, Carney J. beta-Amyloid peptide free radical fragments initiate synaptosomal lipoperoxidation in a sequence-specific fashion: implications to Alzheimer's disease. *Biochem Biophys Res Commun* 1994;200:710–715.
- [46] Blanc EM, Toborek M, Mark RJ, Hennig B, Mattson MP. Amyloid beta-peptide induces cell monolayer albumin permeability, impairs glucose transport, and induces apoptosis in vascular endothelial cells. *J Neurochem* 1997;68:1870–1881.
- [47] Huang X, Cuaungco MP, Atwood CS, Hartshorn MA, Tyndall JD, Hanson GR. Cu(II) potentiation of alzheimer beta neurotoxicity. Correlation with cell-free hydrogen peroxide production and metal reduction. *J Biol Chem* 1999;274:37111–37116.
- [48] Johnstone M, Gearing AJ, Miller KM. A central role for astrocytes in the inflammatory response to beta-amyloid; chemokines, cytokines and reactive oxygen species are produced. *J Neuroimmunol* 1999;93:182–193.



- [49] Esparza JL, Gomez M, Rosa Noguez M, Paternain JL, Mallol J, Domingo JL. Melatonin reduces oxidative stress and increases gene expression in the cerebral cortex and cerebellum of aluminum-exposed rats. *J Pineal Res* 2005;39:129–136.
- [50] Kotler M, Rodriguez C, Sainz RM, Antolin I, Menendez-Pelaez A. Melatonin increases gene expression for antioxidant enzymes in rat brain cortex. *J Pineal Res* 1998;24:83–89.
- [51] Urata Y, Honma S, Goto S, Todoroki S, Iida T, Cho S. Melatonin induces gamma-glutamylcysteine synthetase mediated by activator protein-1 in human vascular endothelial cells. *Free Radic Biol Med* 1999;27:838–847.
- [52] Inselmann G, Blank M, Baumann K. Cyclosporine A induced lipid peroxidation in microsomes and effect on active and passive glucose transport by brush border membrane vesicles of rat kidney. *Res Commun Chem Path Pharm* 1988;62:207–220.
- [53] Mattson MP, Cheng B, Davis D, Bryant K, Lieberburg I, Rydel RE. beta-Amyloid peptides destabilize calcium homeostasis and render human cortical neurons vulnerable to excitotoxicity. *J Neurosci* 1992;12:376–389.
- [54] Mark RJ, Pang Z, Geddes JW, Uchida K, Mattson MP. Amyloid beta-peptide impairs glucose transport in hippocampal and cortical neurons: involvement of membrane lipid peroxidation. *J Neurosci* 1997;17:1046–1054.
- [55] Brera B, Serrano A, de Ceballos ML. beta-amyloid peptides are cytotoxic to astrocytes in culture: a role for oxidative stress. *Neurobiol Dis* 2000;7:395–405.
- [56] Gil-Bea FJ, Garcia-Alloza M, Dominguez J, Marcos B, Ramirez MJ. Evaluation of cholinergic markers in Alzheimer's disease and in a model of cholinergic deficit. *Neurosci Lett* 2005;375:37–41.
- [57] Massoulie J, Pezzementi L, Bon S, Krejci E, Vallette FM. Molecular and cellular biology of cholinesterases. *Progress Neurobiol* 1993;41:31–91.
- [58] Silman I, Sussman JL. Acetylcholinesterase: 'classical' and 'non-classical' functions and pharmacology. *Curr Opin Pharmacol* 2005;5:293–302.
- [59] Sberna G, Saez-Valero J, Beyreuther K, Masters CL, Small DH. The amyloid beta-protein of Alzheimer's disease increases acetylcholinesterase expression by increasing intracellular calcium in embryonal carcinoma P19 cells. *J Neurochem* 1997;69:1177–1184.
- [60] Efanage SM, Garland EM, Staley JK, Khare AB, Mash DC. Vesicular acetylcholine transporter density and Alzheimer's disease. *Neurobiol Aging* 1997;18:407–413.
- [61] Quinlivan M, Chalon S, Vergote J, Henderson J, Katsifis A, Kassiou M, Guillaudeau D. Decreased vesicular acetylcholine transporter and alpha(4)beta(2) nicotinic receptor density in the rat brain following 192 IgG-saporin immunolesioning. *Neurosci Lett* 2007;415:97–101.
- [62] Hoshi M, Takashima A, Murayama M, Yasutake K, Yoshida N, Ishiguro K, Hashino T. Nontoxic amyloid beta peptide 1–42 suppresses acetylcholine synthesis. Possible role in cholinergic dysfunction in Alzheimer's disease. *J Biol Chem* 1997;272:s2038–2041.
- [63] Masilamoni JG, Jesudason EP, Bharathi SN, Jayakumar R. The protective effect of alpha-crystallin against acute inflammation in mice. *Biochim Biophys Acta* 2005;1740:411–420.
- [64] Masilamoni JG, Jesudason EP, Baben B, Jebaraj CE, Dhandayuthapani S, Jayakumar R. Molecular chaperone alpha-crystallin prevents detrimental effects of neuroinflammation. *Biochim Biophys Acta* 2006;1762:284–293.
- [65] Kaneko K, Nakamura A, Yoshida K, Kametani F, Higuchi K, Ikeda S. Glial fibrillary acidic protein is greatly modified by oxidative stress in aceruloplasminemia brain. *Free Radic Res* 2002;36:303–306.
- [66] Eng LF, Ghirnikar RS. GFAP and astrogliosis. *Brain Pathol* 1994;4:229–237.
- [67] Quintana JG, Lopez-Colberg II, Cunningham LA. Use of GFAP-lacZ transgenic mice to determine astrocyte fate in grafts of embryonic ventral midbrain. *Brain Res Dev Brain Res* 1998;105:147–151.
- [68] Tao-Cheng JH, Nagy Z, Brightman MW. Tight junctions of brain endothelium *in vitro* are enhanced by astroglia. *J Neurosci* 1987;7:3293–3299.
- [69] Jesudason EP, Masilamoni JG, Jebaraj CE, Paul SF, Jayakumar R. Efficacy of DL-alpha lipoic acid against systemic inflammation-induced mice: antioxidant defense system. *Mol Cell Biochem* 2008;313:113–123.
- [70] Kondo T, Higashiyama Y, Goto S, Iida T, Cho S, Iwanaga M, Mori K, Tani M, Urata Y. Regulation of gamma-glutamylcysteine synthetase expression in response to oxidative stress. *Free Radic Res* 1999;31:325–334.